

Dalton Transactions

Accepted Manuscript



This is an *Accepted Manuscript*, which has been through the Royal Society of Chemistry peer review process and has been accepted for publication.

Accepted Manuscripts are published online shortly after acceptance, before technical editing, formatting and proof reading. Using this free service, authors can make their results available to the community, in citable form, before we publish the edited article. We will replace this *Accepted Manuscript* with the edited and formatted *Advance Article* as soon as it is available.

You can find more information about *Accepted Manuscripts* in the [Information for Authors](#).

Please note that technical editing may introduce minor changes to the text and/or graphics, which may alter content. The journal's standard [Terms & Conditions](#) and the [Ethical guidelines](#) still apply. In no event shall the Royal Society of Chemistry be held responsible for any errors or omissions in this *Accepted Manuscript* or any consequences arising from the use of any information it contains.

Synthesis, structural characterization, and some properties of 2-acylmethyl-6-ester group-difunctionalized pyridine-containing iron complexes related to active site of [Fe]-hydrogenase[†]

Li-Cheng Song,* Fu-Qiang Hu, Miao-Miao Wang, Zhao-Jun Xie, Kai-Kai Xu and Hai-Bin Song

As biomimetic models for [Fe]-hydrogenase, the 2-acylmethyl-6-ester group-difunctionalized pyridine-containing iron(II) complexes **1–4** have been successfully prepared via the following three separate steps. In the first step, the acylation or esterification of difunctionalized pyridine 2-(*p*-MeC₆H₄SO₃CH₂)-6-HOCH₂C₅H₃N with acetyl chloride or benzoic acid gives the corresponding pyridine derivatives 2-(*p*-MeC₆H₄SO₃CH₂)-6-RCO₂CH₂C₅H₃N (**A**, R = Me; **B**, R = Ph). The second step involves reaction of **A** or **B** with Na₂Fe(CO)₄ followed by treatment of the intermediate Fe(0) complexes [Na(2-CH₂-6-RCO₂CH₂C₅H₃N)]Fe(CO)₄ (**M**₁, R = Me; **M**₂, R = Ph) with iodine to afford 2-acylmethyl-6-acetoxymethyl or 6-benzoyloxymethyl-difunctionalized pyridine-containing Fe(II) iodide complexes [2-C(O)CH₂-6-RCO₂CH₂C₅H₃N]Fe(CO)₂I (**1**, R = Me; **3**, R = Ph). Finally, when **1** or **3** is treated with sodium 2-mercaptopyridinate, the corresponding difunctionalized pyridine-containing Fe(II) mercaptopyridinate complexes [2-C(O)CH₂-6-RCO₂C₅H₃N]Fe(CO)₂(2-SC₅H₄N) (**2**, R = Me; **4**, R = Ph) are produced. While the structures of model complexes **1–4** are confirmed by X-ray crystallography, the electrochemical properties of **2** and **4** are compared with those of the two

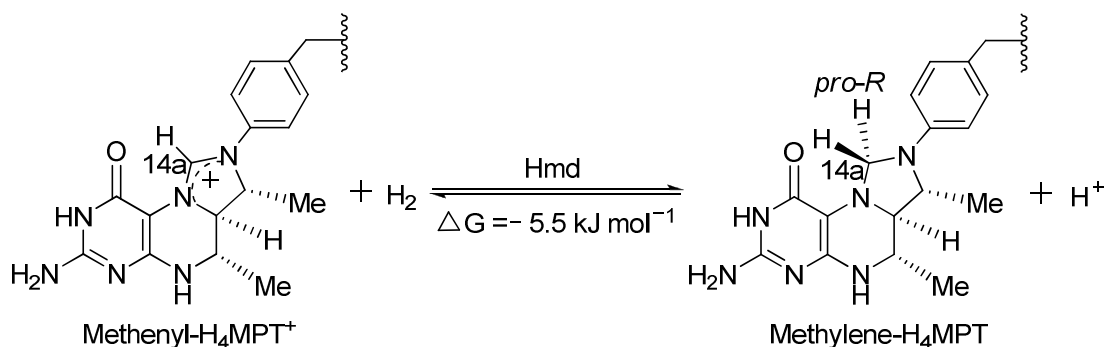
Department of Chemistry, State Key Laboratory of Elemento-Organic Chemistry, and Collaborative Innovation Center of Chemical Science and Engineering (Tianjin), Nankai University, Tianjin 300071, China. E-mail: lcsong@nankai.edu.cn.

[†] CCDC reference numbers 983089-983092. For crystallographic data in CIF see DOI: 10.1039/b000000x/.

previously reported models. In addition, complexes **2** and **4** have been found to be catalysts for H_2 production in the presence of TFA under CV conditions.

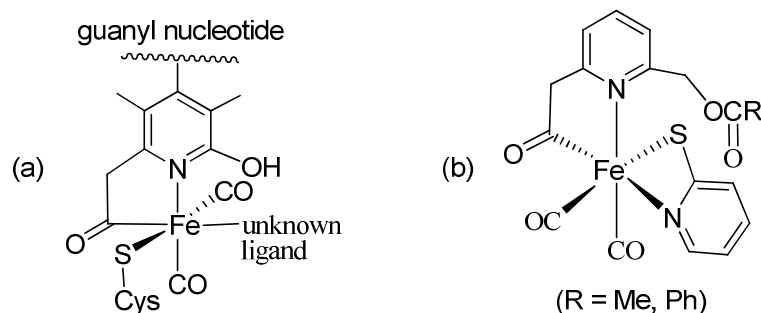
Introduction

Hydrogenases are natural enzymes, which catalyze the reversible H_2 metabolism at high rates in a wide range of microorganisms.¹⁻³ There are three major hydrogenases: [FeFe]-hydrogenases, [NiFe]-hydrogenases, and [Fe]-hydrogenase. While [FeFe]- and [NiFe]-hydrogenases catalyze the reversible redox reaction of hydrogen with protons and electrons,⁴⁻⁶ [Fe]-hydrogenase (also named as Hmd, or iron-sulfur cluster-free hydrogenase) catalyzes the reversible reduction of methenyltetrahydromethanopterin (methenyl- H_4MPT^+) with H_2 to give methylenetetrahydromethanopterin (methylene- H_4MPT) and proton (Scheme 1).^{3,7,8} This stereospecific hydride transfer reaction from H_2 to C_{14a} of methenyl- H_4MPT^+ is an intermediate step in the reduction of CO_2 to methane by methanogens grown under Ni-deficient conditions.⁹



Scheme 1 Reversible hydride transfer catalyzed by [Fe]-hydrogenase.

Spectroscopic¹⁰⁻¹² and particularly X-ray crystallographic¹³⁻¹⁵ studies indicated that [Fe]-hydrogenase contains a unique and intriguing active site, which consists of an iron center ligated by a cysteine S atom, two *cis*-carbonyls, a 2-acylmethyl-6-pyridinol ligand, and an as yet unknown ligand, which is probably a molecule of water (Scheme 2a).



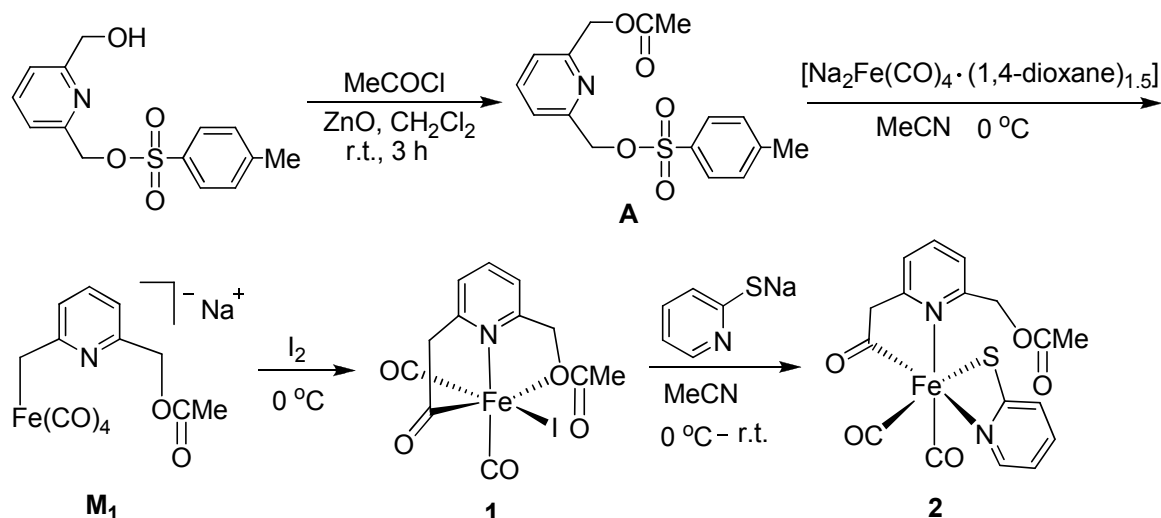
Scheme 2 (a) Proposed active site of [Fe]-hydrogenase. (b) Two representative models reported in this article.

Encouraged by such a well-elucidated structure, numerous Hmd model complexes have been synthesized, so far.¹⁶⁻²⁸ However, among these reported models no one contains the 2-acylmethyl-6-ester group-difunctionalized pyridine ligand, although some of them contain a similar difunctionalized pyridine ligand, such as Hu's acylmethyl/methoxy-difunctionalized,²³⁻²⁵ Pickett's carbamoyl/amino-difunctionalized,²⁹ Chen's acylmethyl/hydroxy-difunctionalized,³⁰ or our acylmethyl/hydroxymethyl-²⁷ and acylmethyl/methoxybenzyl-³¹ difunctionalized pyridine ligands. Therefore, to further understand the active site structure of [Fe]-hydrogenase and to see the influence of the difunctionalized pyridine ligands towards the structure and property of such model complexes, we recently launched a study aimed to synthesize the hitherto unknown 2-acylmethyl-6-ester group-difunctionalized pyridine ligand-containing model complexes. Herein, we report the studied results regarding the synthesis, structural characterization, and some properties of such novel model complexes (Scheme 2b). In addition, the synthesis and characterization of two precursor compounds employed for preparing the model complexes are also described.

Results and discussion

Synthesis and characterization of 2-acylmethyl-6-acetoxymethyl-difunctionalized pyridine-containing model complexes [2-C(O)CH₂-6-MeCO₂CH₂C₅H₃N][Fe(CO)₂I] (1**)/[2-C(O)CH₂-6-MeCO₂CH₂C₅H₃N][Fe(CO)₂(2-SC₅H₄N)] (**2**) and their precursor [2-(*p*-MeC₆H₄SO₃CH₂)-6-MeCO₂CH₂C₅H₃N] (**A**)**

The synthetic route for preparing precursor **A** and model complexes **1** and **2** includes three separate steps as shown in Scheme 3. In the first step precursor **A** is prepared by acylation of 2-(*p*-MeC₆H₄SO₃CH₂)-6-HOCH₂C₅H₃N with acetyl chloride in CH₂Cl₂ in the presence of ZnO in 57% yield. The second step involves reaction of **A** with Na₂Fe(CO)₄ in MeCN followed by treatment of the resulting Fe(0) intermediate [Na(2-CH₂-6-MeCO₂CH₂C₅H₃N)Fe(CO)₄] (**M₁**) with oxidant I₂ (via in situ CO migratory insertion followed by coordination of iodide and the singly-bonded O atom of the ester group with its Fe(0) center) to give the difunctionalized pyridine-containing Fe(II) iodide complex **1** in 40% yield. Finally, in order to obtain a more natural model, **1** was further treated with sodium 2-mercaptopyridinate in MeCN (via nucleophilic substitution of iodide by 2-mercaptopyridinate and subsequent displacement of the singly-bonded O atom by mercaptopyridine N atom) to give the difunctionalized pyridine-containing Fe(II) mercaptopyridinate complex **2** in 59% yield. Actually, the suggested pathway for production of complexes **1** and **2** is very similar to that previously reported for the formation of acylmethyl/hydroxymethyl- and acylmethyl/methoxybenzyl-difunctionalized pyridine-containing model complexes.^{27,31}



In order to prove the suggested pathway starting from precursor **A** to model complex **1**, we utilized in situ IR spectroscopy^{27,32} to monitor the existence of the highly reactive intermediate **M₁** and its in situ conversion under the action of iodide. As shown in Fig. 1, when **A** was added to a MeCN solution of Na₂Fe(CO)₄, the original ν_{CO} absorption bands of Na₂Fe(CO)₄ at 1760 (vs), 1885 (m), and 1916 (w) cm⁻¹ were gradually diminished, and after ca. 10 min, they were completely replaced by a very strong band at 1887 cm⁻¹ and a middle band at 2001 cm⁻¹. This implies that Na₂Fe(CO)₄ was totally consumed and the intermediate **M₁** formed. The in situ IR spectroscopy further demonstrated that after addition of I₂ (ca. 15 min), the aforementioned two ν_{CO} absorption bands disappeared, and instead two middle bands at 2038 and 1978 cm⁻¹ along with two weak bands at 1750 and 1681 cm⁻¹ emerged. The four new bands can be attributed to the two *cis*-arranged terminal carbonyls, one ester carbonyl, and one acyl ligand for the newly formed complex **1**, respectively.

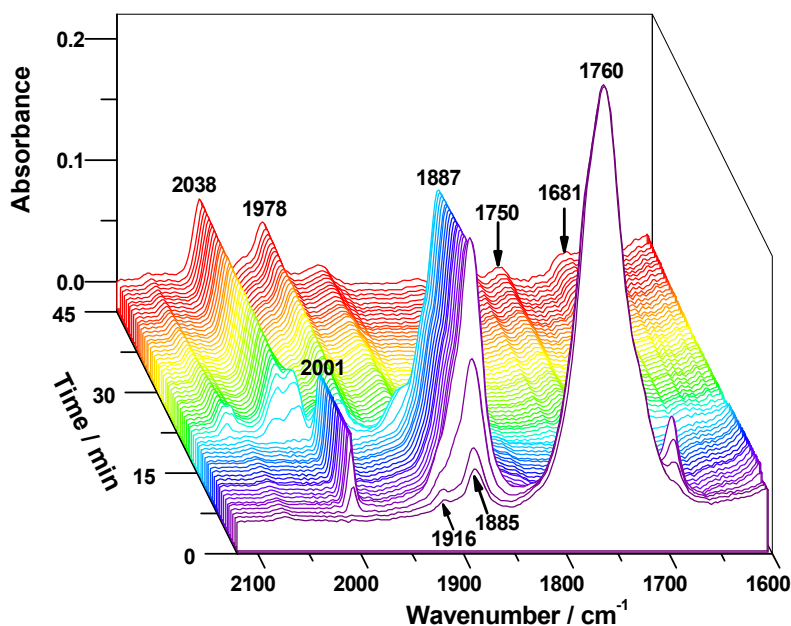


Fig. 1 In situ IR spectra for formation of **1** starting from $\text{Na}_2\text{Fe}(\text{CO})_4$ via intermediate M_1 in MeCN at 0°C .

Compounds **A**, **1**, and **2** are air-stable yellow solids, which have been characterized by elemental analysis and spectroscopy. The solid IR spectrum of **A** showed a very strong absorption band at 1745 cm^{-1} for its ester carbonyl, whereas **1** and **2** showed two strong absorption bands in the range $2030\text{--}1964\text{ cm}^{-1}$ for their two *cis*-arranged terminal carbonyls, one band at 1769 or 1744 cm^{-1} for their ester carbonyl groups, and one band at 1683 or 1656 cm^{-1} for their acyl groups, respectively. The ^1H NMR spectrum of **A** displayed a singlet at 2.45 ppm for CH_3 group attached to its benzene ring and a singlet at 5.13 ppm for the four H atoms in the two methylene groups attached to its pyridine ring, whereas **1** and **2** displayed two doublets in the regions $3.90\text{--}4.65$ and $4.70\text{--}5.65\text{ ppm}$ for their $\text{CH}_2\text{C}=\text{O}$ and $\text{CH}_2\text{OC}=\text{O}$ groups, respectively, since the two H atoms in each of the two groups are diastereotopic. The $^{13}\text{C}\{^1\text{H}\}$ NMR spectrum of **A** showed one signal at 169.5 ppm for its ester carbonyl, whereas **1** and **2** exhibited one signal at 252.2 and 263.2 ppm characteristic of their acyl C atoms attached to their Fe centers,

respectively.^{23,27}

The molecular structures of **1** and **2** were further confirmed by X-ray crystal diffraction analysis. Table 1 lists their selected bond lengths and angles, while their ORTEP views are depicted in Fig. 2 and 3, respectively.

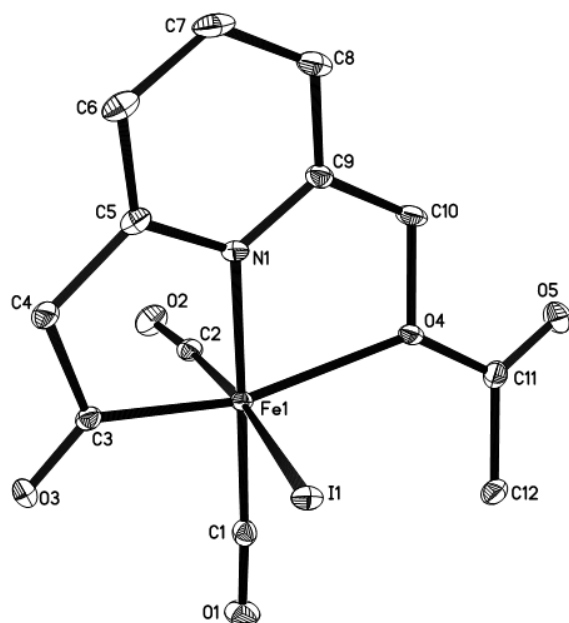


Fig. 2 ORTEP plot of **1** with 30% probability level ellipsoids.

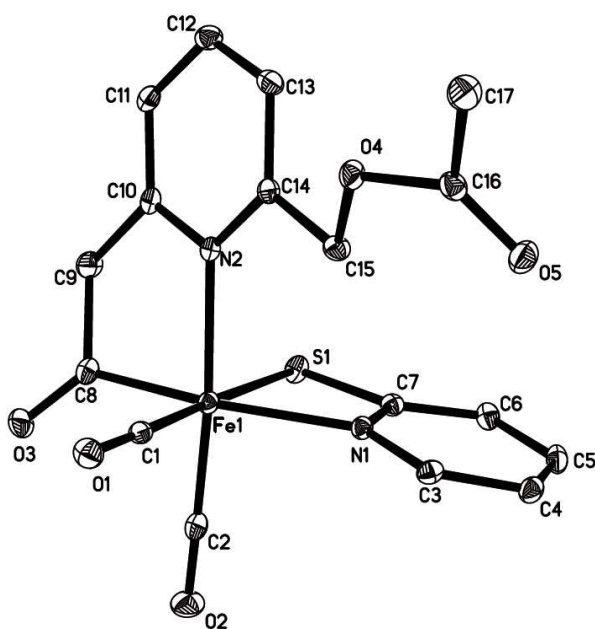


Fig. 3 ORTEP plot of **2** with 30% probability level ellipsoids

Table 1 Selected bond lengths (Å) and angles (°) for **1** and **2**

1			
Fe(1)–C(3)	1.915(2)	O(3)–C(3)	1.202(2)
Fe(1)–N(1)	1.9517(17)	O(5)–C(11)	1.194(3)
Fe(1)–O(4)	2.2537(16)	N(1)–C(9)	1.344(3)
Fe(1)–I(1)	2.6571(9)	N(1)–C(5)	1.350(3)
C(3)–Fe(1)–N(1)	85.81(9)	O(4)–Fe(1)–I(1)	89.33(5)
C(3)–Fe(1)–O(4)	161.41(7)	O(5)–C(11)–C(12)	126.5(2)
N(1)–Fe(1)–O(4)	75.99(7)	C(11)–O(4)–C(10)	113.32(16)
N(1)–Fe(1)–I(1)	89.71(6)	C(4)–C(3)–Fe(1)	110.91(15)
2			
Fe(1)–C(8)	1.9272(18)	O(3)–C(8)	1.2137(19)
Fe(1)–N(2)	2.0538(15)	O(5)–C(16)	1.2009(19)
Fe(1)–N(1)	2.0822(16)	N(2)–C(10)	1.258(2)
Fe(1)–S(1)	2.3699(10)	N(2)–C(14)	1.3494(19)
C(8)–Fe(1)–N(2)	83.42(6)	C(8)–Fe(1)–S(1)	91.69(5)
C(8)–Fe(1)–N(1)	160.98(6)	N(2)–Fe(1)–S(1)	88.14(4)
N(2)–Fe(1)–N(1)	96.53(5)	C(7)–S(1)–Fe(1)	79.82(6)
N(1)–Fe(1)–S(1)	69.32(4)	Fe(1)–C(8)–O(3)	130.33(13)

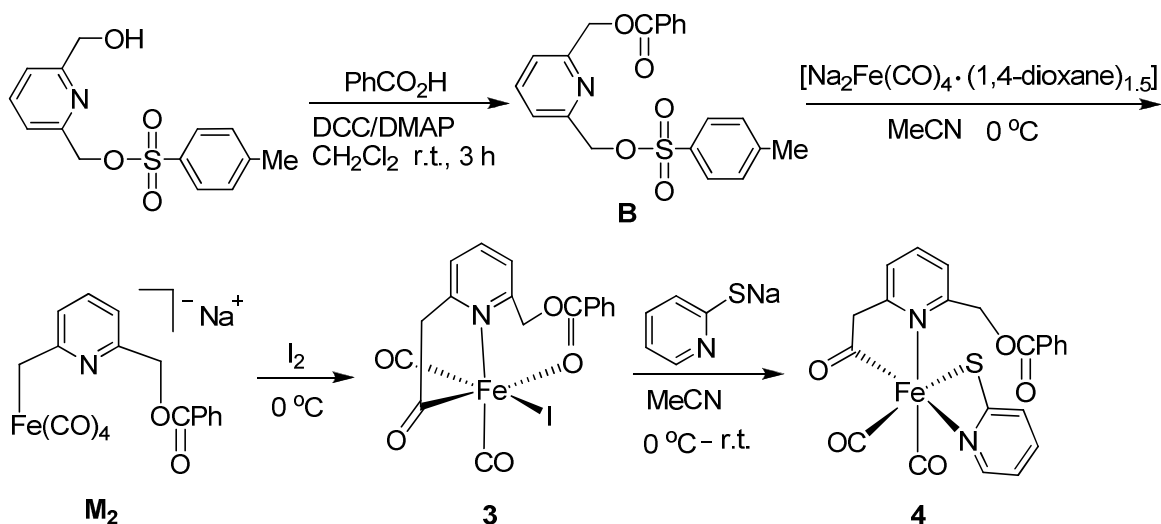
As shown in Fig. 2 and 3, model complexes **1** and **2** indeed contain a difunctionalized 2-acylmethyl-6-acetoxymethyl pyridine ligand. While the difunctionalized pyridine ligand of **1** forms two five-membered (Fe(1)–C(3)–C(4)–C(5)–N(1) and Fe(1)–N(1)–C(9)–C(10)–O(4)) ferrocycles with its iron center, the difunctionalized ligand of **2** forms only one five-membered (Fe(1)–C(8)–C(9)–C(10)–N(2)) ferrocycle since the acetoxymethyl functionality is not

coordinated with Fe(1) center (in **2** there is still another four-membered Fe(1)-S(1)-C(7)-N(1) ferrocycle formed by coordination of its 2-mercaptopyridinate ligand with Fe(1) center). In addition, just like the natural [Fe]-hydrogenase^{14,15} and those previously reported [Fe]-hydrogenase model complexes,^{7,8} both **1** and **2** contain two terminal CO ligands that occupy the positions *cis* to their acylmethyl ligands.

Synthesis and characterization of 2-acylmethyl-6-benzoyloxymethyl-difunctionalized pyridine-containing model complexes [2-C(O)CH₂-6-PhCO₂CH₂C₅H₃N][Fe(CO)₂I] (3**) / [2-C(O)CH₂-6-PhCO₂CH₂C₅H₃N][Fe(CO)₂(2-SC₅H₄N)] (**4**) and their precursor [2-(*p*-MeC₆H₄SO₃CH₂)-6-PhCO₂CH₂C₅H₃N] (**B**)**

In order to observe the influence of 6-ester group upon the structure and property of 2-acylmethyl-6-ester group-difunctionalized pyridine-containing model complexes, we decided (after preparation of the aliphatic ester group-containing complexes **1** and **2**) to prepare the 6-aromatic ester group-containing model complexes **3** and **4**. Actually, model complexes **3/4** and their precursor **B** can be also prepared via the synthetic route similar to that for preparation of their analogues **1/2** and **A**, as shown in Scheme 4. In the first step precursor **B** is prepared by esterification reaction of 2-(*p*-MeC₆H₄SO₃CH₂)-6-HOCH₂C₅H₃N with benzoic acid under the action of DCC (as an activator) and DMAP (as a catalyst) in 85% yield. The second step includes reaction of **B** with Na₂Fe(CO)₄ in MeCN followed by treatment of the resulting Fe(0) complex salt [Na(2-CH₂-6-PhCO₂CH₂C₅H₃N)Fe(CO)₄] (**M₂**) with iodine, via in situ CO migratory insertion followed coordination of iodide and the doubly-bonded O atom (note that not the singly-bonded O atom) of the ester group with its Fe(0) center, to afford the difunctionalized pyridine-containing Fe(II) iodide complex **3** in 38% yield. Finally, the difunctionalized pyridine-

containing Fe(II) mercaptopyridinate complex **4** is produced in 62% yield by reaction of **3** with sodium 2-mercaptopyridinate through nucleophilic substitution of the doubly-bonded O atom by mercaptopyridine N atom.



Compounds **B**, **3**, and **4** are also air-stable solids. The solid IR spectrum of **B** displayed a very strong absorption band at 1722 cm^{-1} for its ester carbonyl, whereas **3** and **4** exhibited two very strong absorption bands in the range $2036\text{--}1964\text{ cm}^{-1}$ for their two terminal carbonyls, one band at 1655 or 1657 cm^{-1} for their acyl groups, and one band at 1683 or 1723 cm^{-1} for their ester carbonyl groups, respectively. The ^1H NMR spectrum of **B** exhibited a singlet at 2.43 ppm assigned for its CH_3 group and two singlets at 5.15 and 5.40 ppm for its CH_2OSO_2 and $\text{CH}_2\text{OC=O}$ groups, respectively, whereas the ^1H NMR spectra of **3** and **4** displayed two doublets in the range $3.90\text{--}4.65\text{ ppm}$ and two doublets in the range $4.90\text{--}5.85\text{ ppm}$ for their $\text{CH}_2\text{C=O}$ and $\text{CH}_2\text{OC=O}$ groups since the two H atoms in the two groups are diastereotopic. The $^{13}\text{C}\{^1\text{H}\}$ NMR spectrum of **B** showed one singlet at 166.1 ppm for its ester carbonyl, whereas the $^{13}\text{C}\{^1\text{H}\}$ NMR spectra of **3** and **4** each displayed a signal at 252.3 and 262.8 ppm typical of their acyl carbon atoms, respectively.

The X-ray crystallographic study (Fig. 4 and 5, Table 2) indicated that both **3** and **4** have a difunctionalized 2-acylmethyl-6-benzoyloxymethyl pyridine ligand. While the difunctionalized pyridine ligand of **3** constructs a five-membered (Fe(1)-C(3)-C(4)-C(5)-N(1)) ferrocycle and a seven-membered (Fe(1)-N(1)-C(9)-C(10)-O(4)-C(11)-O(5)) ferrocycle that is generated by coordination of the doubly-bonded O(5) atom of the 2-acylmethyl-6-benzoyloxymethyl ligand, the difunctionalized pyridine ligand of **4** constructs only one five-membered Fe(1)-C(3)-C(4)-C(5)-N(1) ferrocycle with Fe(1) center since the benzoyloxymethyl functionality is like the acetoxymethyl functionality in its analogue **2** not to coordinate with Fe center. In addition, both **3** and **4** also have two terminal CO ligands *cis* to their acylmethyl ligands, whereas complex **4** has an additional four-membered Fe(1)-S(1)-C(18)-N(2) ferrocycle constructed by coordination of its 2-mercaptopyridinate ligand with Fe(1) center. It follows that the structures of model complexes **3** and **4** are very similar to those of their analogues **1** and **2** as well as the active site of [Fe]-hydrogenase.^{14,15}

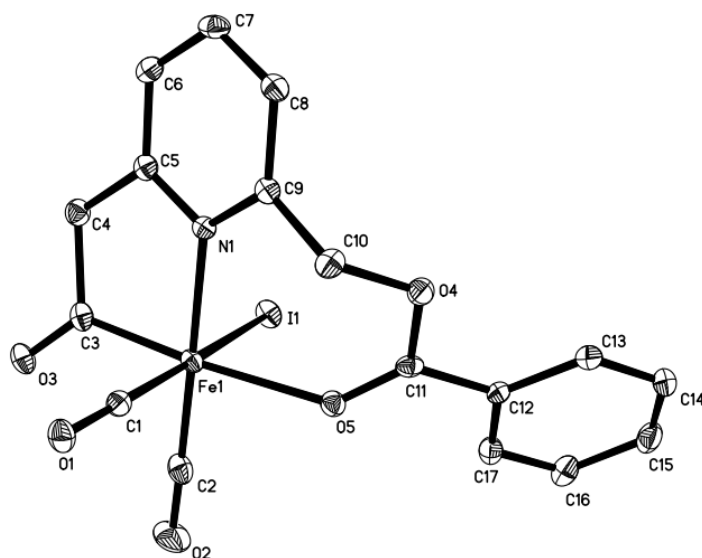


Fig. 4 ORTEP plot of **3** with 30% probability level ellipsoids.

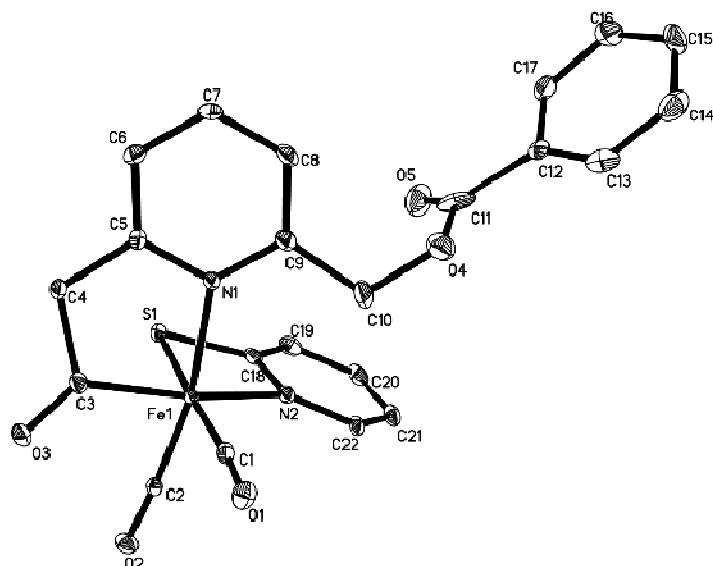


Fig. 5 ORTEP plot of **4** with 30% probability level ellipsoids.

Table 2 Selected bond lengths (Å) and angles (°) for **3** and **4**

3			
Fe(1)–I(1)	2.6749(8)	O(3)–C(3)	1.211(2)
Fe(1)–C(3)	1.914(2)	O(4)–C(11)	1.340(2)
Fe(1)–N(1)	2.0173(15)	O(5)–C(11)	1.216(2)
Fe(1)–O(5)	2.1589(14)	N(1)–C(5)	1.350(2)
C(3)–Fe(1)–N(1)	85.18(7)	N(1)–Fe(1)–I(1)	92.29(4)
C(3)–Fe(1)–O(5)	171.67(7)	O(5)–Fe(1)–I(1)	86.11(4)
N(1)–Fe(1)–O(5)	93.58(6)	C(11)–O(4)–C(10)	115.89(15)
C(3)–Fe(1)–I(1)	85.71(6)	C(11)–O(5)–Fe(1)	138.35(12)
4			
N(1)–C(9)	1.365(5)	O(5)–C(11)	1.178(5)
Fe(1)–N(2)	2.084(3)	N(1)–C(5)	1.351(4)
Fe(1)–N(1)	2.079(3)	N(2)–C(18)	1.350(5)
Fe(1)–S(1)	2.3823(11)	N(2)–C(22)	1.350(5)
C(3)–Fe(1)–N(2)	161.65(13)	C(3)–Fe(1)–S(1)	92.47(10)

C(3)–Fe(1)–N(1)	82.88(14)	N(2)–Fe(1)–S(1)	69.24(8)
N(2)–Fe(1)–N(1)	97.95(11)	C(18)–S(1)–Fe(1)	79.56(12)
N(1)–Fe(1)–S(1)	89.34(9)	Fe(1)–C(3)–O(3)	130.7(3)

Electrochemical behavior of model complexes **2** and **4**

Although the electrochemistry of many [FeFe]-hydrogenase model complexes have been well-studied,^{32–36} very few [Fe]-hydrogenase model complexes are electrochemically investigated to date.^{29,37} To make a comparison with the electrochemical behavior of the previously reported Hmd models^{29,37} and thus to see the influences of the ligands around their iron centers, we determined the electrochemical properties of model complexes **2** and **4** by cyclic voltammetric techniques. The cyclic voltammograms of **2** and **4** are shown in Fig. 6, whereas Table 3 lists their electrochemical data along with those of the previously reported model complexes FeBr(2-acylaminopyridine)(CO)₂(PMe₃) (**C**)²⁹ and Fe(3,6-dichloro-1,2-benzenedithiolate)(CO)₂(PMe₃)₂ (**D**).³⁷ As shown in Fig. 6 and Table 3, both **2** and **4** display one irreversible reduction at $E_{\text{pc1}} = -1.86/-1.85$ V and one irreversible oxidation at $E_{\text{pa}} = +0.60/+0.68$ V versus Fc/Fc⁺, respectively. In addition, as shown in Table 3, the electrochemical behavior of complexes **2** and **4** is very similar to that of the previously reported complex **C**. For example, they all display one irreversible reduction and one irreversible oxidation at their respective potentials in close proximity due to their structural similarity. However, in contrast to this, the electrochemical behavior of **2** and **4** is considerably different from that of **D**. For example, complex **D** exhibits two irreversible reductions and one reversible oxidation, and particularly the two peak potentials $E_{\text{pc1}}/E_{\text{pa}}$ are greatly shifted negatively to ca. 290–580 mV relative to the corresponding two potentials of **2** and **4**. Apparently, such remarkably different electrochemical behavior between **2/4** and **D** is caused by their quite different structures in which the two strong electron-donating

PMe₃ ligands present in **D** might play a key role for the greatly negative shift of its two redox potentials when compared to those of **2** and **4**.

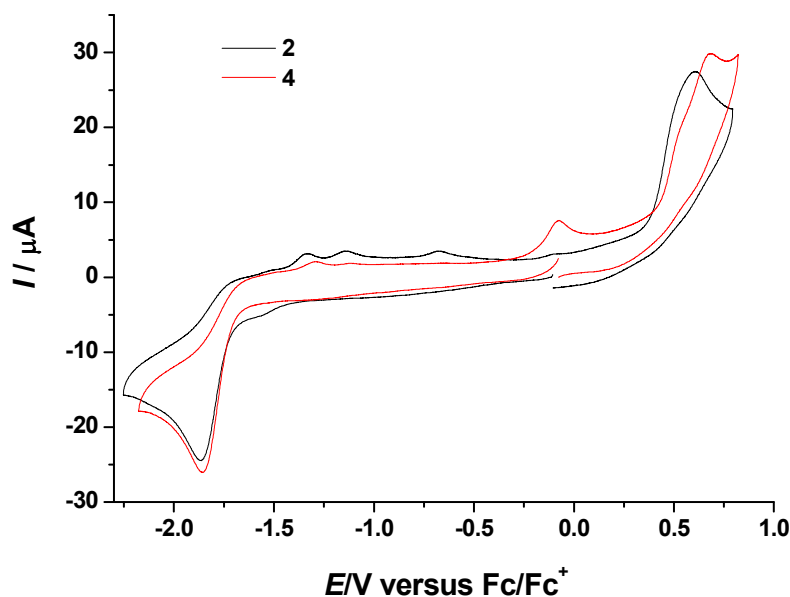


Fig. 6 Cyclic voltammograms of **2** and **4** (1.0 mM) in 0.1 M *n*-Bu₄NPF₆-MeCN at a scan rate of 0.1 V s⁻¹.

Table 3 Electrochemical data of **2**, **4**, **C**, and **D**^a

	E_{pc1}/V	E_{pc2}/V	E_{pa}/V
2	-1.86	----	+0.60
4	-1.85	----	+0.68
C	-1.87	----	+0.75
D	-2.15	-2.34	+0.10

^a All potentials versus Fc/Fc⁺.

In order to observe if complexes **2** and **4** could be able to catalyze proton reduction to H₂, we further determined their cyclic voltammograms in the presence of trifluoroacetic acid (TFA). As shown in Fig. 7 and 8 (For comparison, their cyclic voltammograms without TFA were also included), when TFA was added, the current intensity of the original reduction peaks of **2** and **4**

increased obviously and continued to increase considerably with addition of the acid. Such a remarkable increase of the acid-induced currents could be ascribed to the electrocatalytic proton reduction processes.^{34,36}

The electrocatalytic proton reduction catalyzed by **2** and **4** was further confirmed by a combination of controlled potential electrolysis and GC analysis. When a MeCN solution of **2** or **4** (0.5 mM) was electrolyzed with a large excess TFA (15 mM) at -2.0 V for 0.5 h, a total of 20.6 F mol^{-1} of **2** and 29.0 F mol^{-1} of **4** passed, which correspond to 10.3 and 14.5 turnovers (Note that the turnovers for the controlled potential electrolysis of TFA catalyzed by complex **D** at -1.7 V for 0.5 h were reported to be about 8).³⁷ Gas chromatographic analysis showed that the yields of H_2 evolved in the cases catalyzed by **2** and **4** are all about 95%.

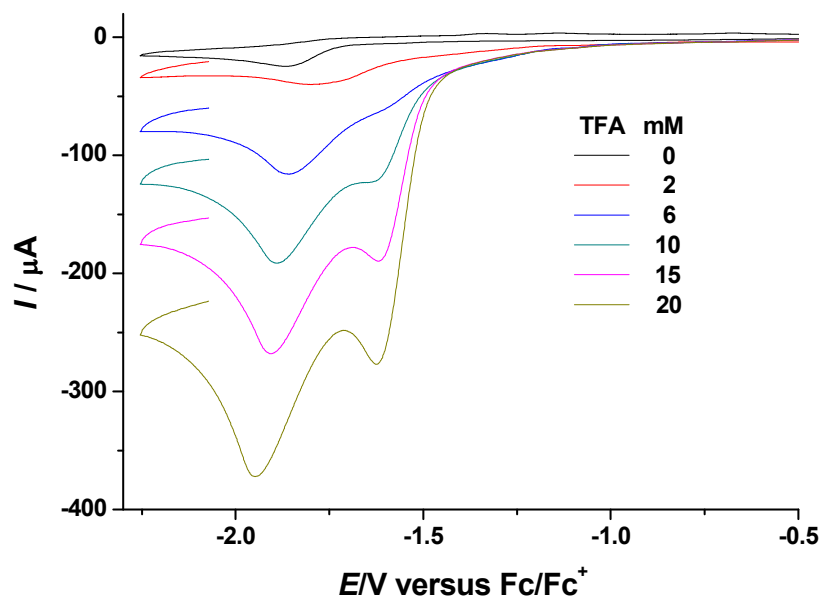


Fig. 7 Cyclic voltammograms of **2** (1.0 mM) with TFA (0–20 mM) in 0.1 M $n\text{-Bu}_4\text{NPF}_6\text{-MeCN}$ at a scan rate of 0.1 V s^{-1} (Reverse scans were partly truncated for clarity).

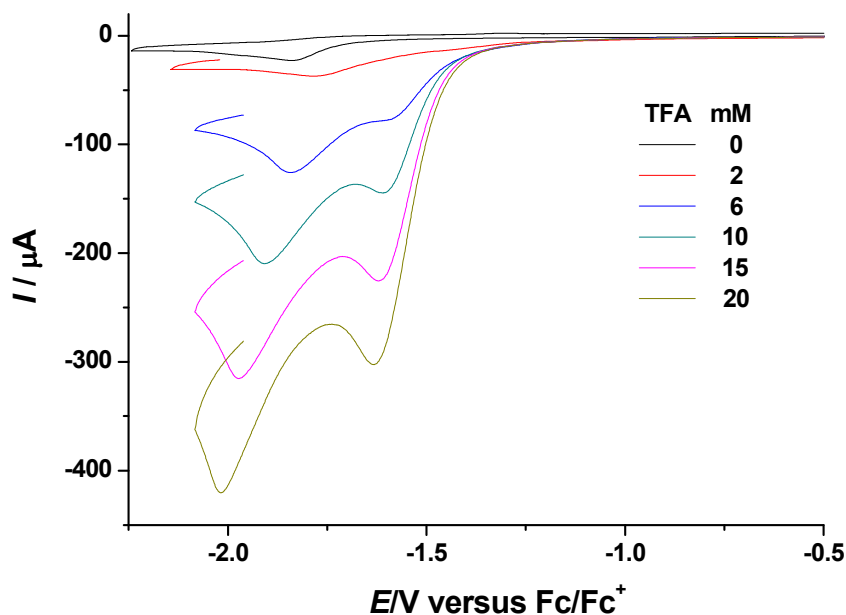


Fig. 8 Cyclic voltammograms of **4** (1.0 mM) with TFA (0–20 mM) in 0.1 M *n*-Bu₄NPF₆–MeCN at a scan rate of 0.1 V s^{−1} (Reverse scans were partly truncated for clarity).

Attempted H₂ activation by model complexes **2** and **4** in the presence of lewis acid Ph₃B or Ph₃C⁺ cation

As the H₂ activation by [Fe]-hydrogenase occurs in the presence of the hydride acceptor (methenyl-H₄MPT⁺),^{3,7,8} we attempted to activate H₂ by our model complexes **2** and **4** in the presence of Lewis acid Ph₃B or carbocation Ph₃C⁺. Initially, we found that when the Ph₃C⁺ cation as its Ph₃C⁺BF₄[−] salt was added to the NMR tube containing an acetone-*d*₆ solution of **2** or **4**, the original ¹H NMR spectra of **2** and **4** were greatly changed. This means that both **2** and **4** were seriously decomposed in the presence of the strong Lewis acid Ph₃C⁺ cation.³⁸ So, we had to use the weaker boron-based Lewis acid Ph₃B³⁹ to test whether models **2** and **4** could activate H₂ or not. For this purpose, the sample solutions were prepared by addition of Ph₃B to the NMR tube containing an acetone-*d*₆ solution of **2** or **4** followed by purging the solutions with H₂ and D₂. As shown in Fig. 9 and 10, the ¹H NMR spectra of the two sample solutions all displayed one singlet at 4.54 ppm for H₂,⁴⁰ four doublets in the region 3.93–5.80 ppm for the diastereotopic

methylene hydrogen atoms in $\text{CH}_2\text{C}=\text{O}$ and $\text{CH}_2\text{OC}=\text{O}$ groups of complex **2** or **4** and the multiplets in the range 6.77–8.46 ppm attributed to the hydrogen atoms of the pyridine and benzene rings present in **2**, **4**, and Ph_3B . In addition, the sample solution containing complex **2** showed a singlet at 2.07 ppm for its CH_3 group. Apparently, these observations demonstrate that complexes **2** and **4** cannot heterolytically activate H_2 and D_2 in the presence of Lewis acid Ph_3B , since no ^1H NMR signal for H-D was detected (Note that the H-D signal is a triplet at 4.57 ppm with $J = 42.51$ Hz).^{40,41}

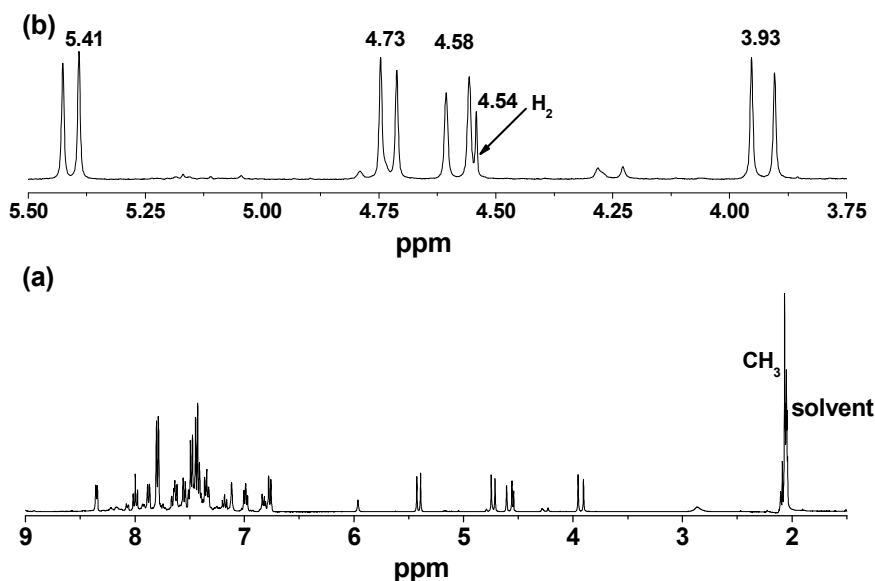


Fig. 9 (a) Original ^1H NMR spectrum of the sample solution consisting of **2**, Ph_3B , H_2 , and D_2 in acetone- d_6 . (b) The expanded ^1H NMR spectrum in the range 3.75–5.50 ppm.

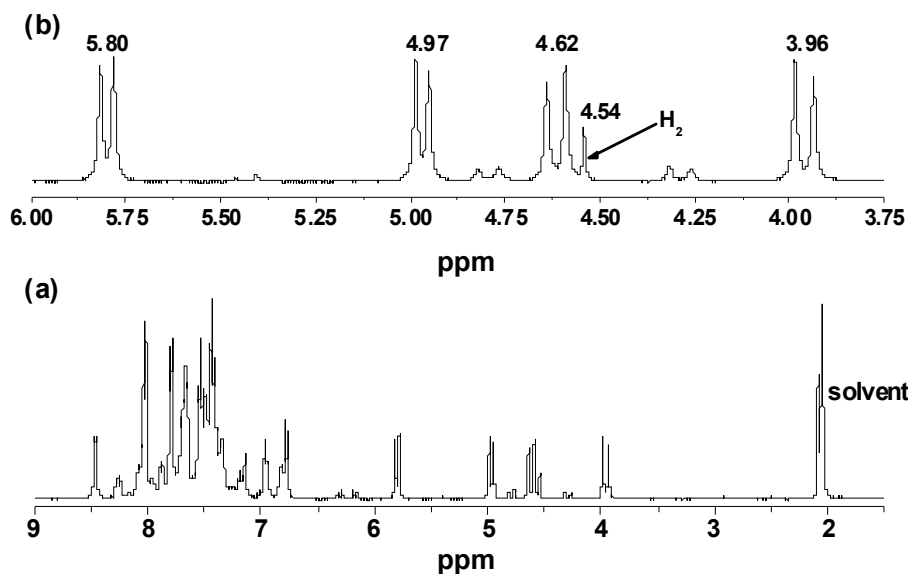


Fig. 10 (a) Original ^1H NMR spectrum of the sample solution consisting of **4**, Ph_3B , H_2 , and D_2 in acetone- d_6 . (b) The expanded ^1H NMR spectrum in the range 3.75–6.00 ppm.

Conclusions

We have synthesized the first [Fe]-hydrogenase model complexes **1–4** each with a 2-acylmethyl-6-ester group-difunctionalized pyridine ligand. While **1** and **2** contains a 2-acylmethyl-6-acetoxymethyl-difunctionalized pyridine ligand, **3** and **4** contains a 2-acylmethyl-6-benzoyloxymethyl-difunctionalized pyridine ligand. The synthetic route to model complexes **1–4** include three separate steps: (i) preparation of new precursor compounds **A** and **B** by reaction of 2-(*p*- $\text{MeC}_6\text{H}_4\text{SO}_3\text{CH}_2$)-6- $\text{HOCH}_2\text{C}_5\text{H}_3\text{N}$ with MeCOCl in the presence of ZnO , or with PhCO_2H in the presence of DCC and DMAP; (ii) preparation of complexes **1** and **3** via reaction of **A** or **B** with $\text{Na}_2\text{Fe}(\text{CO})_4$ followed by treatment of intermediate **M**₁ or **M**₂ with oxidant I_2 ; and (iii) preparation of complexes **2** and **4** by reaction of **1** or **3** with sodium 2-mercaptopyridinate. X-ray crystallographic study reveals that model complexes **1–4** have some common structural features with the active site of [Fe]-hydrogenase, such as (i) they all contain a 2-acylmethyl-6-functionalized pyridine ligand; (ii) all the 2,6-difunctionalized pyridine ligands in **1–4** form a five-membered ferrocycle with their single Fe(II) centers; and (iii) they all have two terminal CO

ligands that are *cis* to their acyl ligands. Actually, model complexes **2** and **4** are structurally more like the active site of [Fe]-hydrogenase than **1** and **3** since they have a sulfur atom located at the fifth coordination site of their Fe(II) centers. It is worth noting that the reaction pathway from precursor **A** to model complex **1** via the highly reactive intermediate **M**₁ is monitored and proved by using in situ IR spectroscopy. In addition, the ¹H NMR spectroscopic study indicates that complexes **2** and **4** cannot activate H₂ and D₂ in the presence of Lewis acid Ph₃B, whereas complexes **2** and **4** have been found to be catalysts for proton reduction to hydrogen in the presence of TFA under CV conditions.

Experimental section

General comments

All reactions were carried out using standard Schlenk and vacuum-line techniques under an atmosphere of highly purified nitrogen. Acetonitrile and dichloromethane were purified by distillation over CaH₂ prior to use. N,N'-dicyclohexylcarbodiimide (DCC) and *p*-dimethylaminopyridine (DMAP), 2-mercaptopyridine, Ph₃B, H₂, D₂, and some other materials were available commercially and used as received. Na₂Fe(CO)₄·(1,4-dioxane)_{1.5},⁴² 2-(*p*-MeC₆H₄SO₃CH₂)-6-HOCH₂C₅H₃N⁴³ and Ph₃C⁺BF₄⁻⁴⁴ were prepared according to the published procedures. Solid IR spectra were recorded on a Bruker Tenser 27 FT-IR spectrophotometer, whereas in situ IR spectra were taken on ReactIR iC10 from Mettler-Toledo AutoChem fitted with a silicon-tipped (SiComp) probe. ¹H (¹³C) NMR spectra were obtained on a Bruker Avance 400 NMR spectrometer. Elemental analyses were performed on an Elementar Vario EL analyzer. Melting points were determined on a SGW X-4 microscopic melting point apparatus and were uncorrected.

Preparation of 2-(*p*-MeC₆H₄SO₃CH₂)-6-MeCO₂CH₂C₅H₃N (**A**)

Acetyl chloride (1.40 mL, 20.00 mmol) was added dropwise to a stirred pink mixture consisting of 2-(*p*-MeC₆H₄SO₃CH₂)-6-HOCH₂C₅H₃N (2.800 g, 9.50 mmol) and ZnO (0.406 g, 5.00 mmol) in CH₂Cl₂ (100 mL). The new mixture was stirred at room temperature for 3 h to give a white suspension. The suspension was washed with a saturated aqueous solution of sodium bicarbonate (20 mL) and water (2 × 10 mL) successively. After the separated organic phase was dried over anhydrous magnesium sulfate, solvent was removed at reduced pressure to leave a residue, which was subjected to TLC separation by using CH₂Cl₂-ethyl acetate (2:1, v/v) as an eluent. From the main band, **A** (1.820 g, 57%) was obtained as a pink solid, mp 54–55 °C. Anal. Calcd for C₁₆H₁₇NO₅S: C, 57.30; H, 5.11; N, 4.18. Found: C, 57.07; H, 5.24; N, 4.21. IR (KBr disk): $\nu_{\text{C=O}}$ 1745 (vs) cm⁻¹. ¹H NMR (400 MHz, CDCl₃): 2.15 (s, 3H, CH₃CO₂), 2.45 (s, 3H, CH₃C₆H₄), 5.13 (s, 4H, 2CH₂), 7.27–7.39 (m, 4H, C₆H₄), 7.72 (t, *J* = 7.8 Hz, 1H, 4-H of C₅H₃N), 7.83 (d, *J* = 7.6 Hz, 2H, 3, 5-H of C₅H₃N) ppm. ¹³C{¹H} NMR (100 MHz, CDCl₃): 19.9 (CH₃CO₂), 20.6 (CH₃C₆H₄), 65.4 (CH₂OSO₂), 70.5 (CH₂OC=O), 119.8, 120.3, 127.1, 128.9, 131.6, 136.8, 144.1, 152.6, 154.4 (C₆H₄, C₅H₃N), 169.5 (CH₂OC=O) ppm.

Preparation of 2-(*p*-MeC₆H₄SO₃CH₂)-6-PhCO₂CH₂C₅H₃N (**B**)

A pink mixture consisting of 2-(*p*-MeC₆H₄SO₃CH₂)-6-HOCH₂C₅H₃N (1.732 g, 6.00 mmol), benzoic acid (1.465 g, 12.00 mmol), DCC (1.800 g, 8.00 mmol), DMAP (0.072 g, 0.60 mmol) in CH₂Cl₂ (10 mL) was stirred at room temperature for 4 h to give a white suspension. After the same workup as that for **A**, from the main band **B** (2.040 g, 85%) was obtained as a white solid, mp 64–65 °C. Anal. Calcd for C₂₁H₁₉NO₅S: C, 63.46; H, 4.82; N, 3.52. Found: C, 63.53; H, 4.64; N, 3.69. IR (KBr disk): $\nu_{\text{C=O}}$ 1722 (vs) cm⁻¹. ¹H NMR (400 MHz, CDCl₃): 2.43 (s, 3H,

CH₃), 5.15 (s, 2H, CH₂OSO₂), 5.40 (s, 2H, CH₂OC=O), 7.33 (d, $J = 7.6$ Hz, 2H, 3,5-H of C₆H₄), 7.38 (d, $J = 8.0$ Hz, 2H, 2,6-H of C₆H₄), 7.46 (t, $J = 7.6$ Hz, 2H, 3,5-H of C₆H₅), 7.59 (t, $J = 7.4$ Hz, 1H, 4-H of C₆H₅), 7.73 (t, $J = 7.8$ Hz, 1H, 4-H of C₅H₃N), 7.83 (d, $J = 8.0$ Hz, 2H, 3,5-H of C₅H₃N), 8.09 (d, $J = 7.6$ Hz, 2H, 2,6-H of C₆H₅) ppm. ¹³C{¹H} NMR (100 MHz, CDCl₃): 21.7 (CH₃), 66.8 (CH₂OSO₂), 71.6 (CH₂OC=O), 120.9, 121.2, 128.1, 128.5, 129.8, 130.0, 132.8, 133.3, 137.9, 145.1, 153.6, 155.8 (C₆H₅, C₆H₄, C₅H₃N), 166.1 (CH₂OC=O) ppm.

Preparation of [2-C(O)CH₂-6-MeCO₂CH₂C₅H₃N]Fe(CO)₂I (1)

A suspension of Na₂Fe(CO)₄·(1,4-dioxane)_{1.5} (173 mg, 0.5 mmol) in MeCN (15 mL) was cooled to 0 °C, and then 2-(*p*-MeC₆H₄SO₃CH₂)-6-MeCO₂CH₂C₅H₃N (**A**) (167 mg, 0.5 mmol) was added. After the mixture was stirred at this temperature for 1 h, I₂ (127 mg, 0.5 mmol) was added, and then the new mixture was stirred at 0 °C for an additional 1 h to give a brown solution. After volatiles were removed at reduced pressure, the residue was subjected to column chromatography (silica gel). Elution with CH₂Cl₂-acetone (40:1, v/v) developed a major yellow band, from which **1** (86 mg, 40%) was obtained as a yellow solid, mp 121 °C (dec). Anal. Calcd for C₁₂H₁₀FeINO₅: C, 33.44; H, 2.34; N, 3.25. Found: C, 33.61; H, 2.51; N, 3.13. IR (KBr disk): $\nu_{\text{C}\equiv\text{O}}$ 2030 (vs), 1966 (vs); $\nu_{\text{C}=\text{O}}$ 1769 (s), 1683 (s) cm⁻¹. ¹H NMR (400 MHz, acetone-*d*₆): 2.39 (s, 3H, CH₃), 4.49, 4.63 (dd, AB system, $J = 20.4$ Hz, 2H, CH₂C=O), 5.55, 5.62 (dd, AB system, $J = 14.4$ Hz, 2H, CH₂OC=O), 7.74 (br s, 2H, 3,5-H of C₅H₃N), 8.14 (br s, 1H, 4-H of C₅H₃N) ppm. ¹³C{¹H} NMR (100 MHz, acetone-*d*₆): 22.9 (CH₃), 64.5 (CH₂C=O), 69.8 (CH₂OC=O), 122.5, 123.2, 141.2, 156.2, 161.2 (C₅H₃N), 171.1 (CH₂OC=O), 210.4, 213.1 (C≡O), 252.2 (CH₂C=O) ppm.

Preparation of [2-C(O)CH₂-6-MeCO₂CH₂C₅H₃N]Fe(CO)₂(2-SC₅H₄N) (**2**)

To a solution of complex [2-C(O)CH₂-6-MeCO₂CH₂C₅H₃N]Fe(CO)₂I (**1**) (172 mg, 0.40 mmol) in MeCN (20 mL) was added 2-NaSC₅H₄N (53 mg, 0.40 mmol). The mixture was stirred at room temperature for 2 h to give a brown solution. After volatiles were removed at reduced pressure, the residue was subjected to column chromatography (silica gel). Elution with CH₂Cl₂-acetone (20:1, v/v) developed a major yellow band, from which **2** (97 mg, 59%) was obtained as a yellow solid, mp 130–132 °C. Anal. Calcd for C₁₇H₁₄FeN₂O₅S: C, 49.29; H, 3.41; N, 6.76. Found: C, 49.25; H, 3.34; N, 6.56. IR (KBr disk): $\nu_{\text{C}\equiv\text{O}}$ 2027 (s), 1964 (s); $\nu_{\text{C}=\text{O}}$ 1744 (m), 1656 (s) cm⁻¹. ¹H NMR (400 MHz, acetone-*d*₆): 2.07 (s, 3H, CH₃), 3.93, 4.58 (dd, *J* = 20.0 Hz, 2H, CH₂C=O), 4.73, 5.41 (dd, *J* = 13.6 Hz, 2H, CH₂OC=O), 6.77 (d, *J* = 8.0 Hz, 1H, 3-H of C₅H₄N), 6.99 (t, *J* = 6.4 Hz, 1H, 5-H of C₅H₄N), 7.48 (t, *J* = 7.8 Hz, 1H, 4-H of C₅H₄N), 7.63 (d, *J* = 7.6 Hz, 1H, 3-H of C₅H₃N), 7.55 (d, *J* = 8.0 Hz, 1H, 5-H of C₅H₃N), 8.00 (t, *J* = 7.6 Hz, 1H, 4-H of C₅H₃N), 8.35 (d, *J* = 4.8 Hz, 1H, 6-H of C₅H₄N) ppm. ¹³C{¹H} NMR (100 MHz, acetone-*d*₆): 20.7 (CH₃), 63.8 (CH₂C=O), 67.2 (CH₂OC=O), 118.9, 122.6, 123.6, 125.9, 137.0, 139.6, 152.5, 159.8, 163.9, 170.6 (C₅H₃N, C₅H₄N), 177.7 (CH₂OC=O), 209.8 (C≡O), 214.42 (C≡O), 263.2 (CH₂C=O) ppm.

Preparation of [2-C(O)CH₂-6-PhCO₂CH₂C₅H₃N]Fe(CO)₂I (**3**)

It was prepared by the same procedure as complex **1**, except that **A** was replaced by 2-(*p*-MeC₆H₄SO₃CH₂)-6-PhCO₂CH₂C₅H₃N (**B**) (198 mg, 0.50 mmol). **3** (94 mg, 38%) was obtained as a yellow solid, mp 136 °C (dec). Anal. Calcd for C₁₇H₁₂FeINO₅: C, 41.25; H, 2.85; N, 2.83. Found: C, 41.44; H, 2.96; N 3.01. IR (KBr disk): $\nu_{\text{C}\equiv\text{O}}$ 2036 (vs), 1969 (vs); $\nu_{\text{C}=\text{O}}$ 1683 (m), 1655 (s) cm⁻¹. ¹H NMR (400 MHz, acetone-*d*₆): 4.35, 4.63 (dd, AB system, *J* = 20.8 Hz, 2H,

CH₂C=O), 5.69, 5.85 (dd, AB system, $J = 13.6$ Hz, 2H, CH₂OC=O), 7.58–8.19 (m, 8H, C₆H₅, C₅H₃N) ppm. ¹³C{¹H} NMR (100 MHz, acetone-*d*₆): 62.5 (CH₂C=O), 67.3 (CH₂OC=O), 122.3, 123.9, 128.8, 129.2, 130.3, 134.4, 139.6, 155.3, 161.5 (C₆H₅, C₅H₃N), 170.7 (CH₂OC=O), 209.6, 211.2 (C≡O), 252.3 (CH₂C=O) ppm.

Preparation of [2-C(O)CH₂-6-PhCO₂CH₂C₅H₃N]Fe(CO)₂(2-C₅H₄NS) (4)

It was prepared by the same procedure as that for complex **2**, but complex [2-C(O)CH₂-6-PhCO₂CH₂C₅H₃N]Fe(CO)₂I (**3**) (200 mg, 0.4 mmol) was used instead of **1**. From the main band complex **4** (118 mg, 62%) was obtained as a brown yellow solid, mp 105–106 °C. Anal. Calcd for C₂₂H₁₆FeN₂O₅S: C, 55.48; H, 3.39; N, 5.88. Found: C, 55.25; H, 3.38; N, 6.03. IR (KBr disk): $\nu_{\text{C=O}}$ 2028 (s), 1964 (s); $\nu_{\text{C=O}}$ 1723 (s), 1657 (s) cm⁻¹. ¹H NMR (400 MHz, acetone-*d*₆): 3.96, 4.61 (dd, $J = 20$ Hz, 2H, CH₂C=O), 4.97, 5.80 (dd, $J = 14$ Hz, 2H, CH₂OC=O), 6.77 (d, $J = 8.4$ Hz, 1H, 3-H of C₅H₄N), 6.96 (t, $J = 6.0$ Hz, 1H, 5-H of C₅H₄N), 7.41 (t, $J = 7.6$ Hz, 1H, 4-H of C₅H₄N), 7.52–7.71 (m, 5H, C₆H₅), 8.02–8.06 (m, 3H, 3,4,5-H of C₅H₃N), 8.46 (d, $J = 4.4$ Hz, 1H, 6-H of C₅H₄N) ppm. ¹³C{¹H} NMR (100 MHz, acetone-*d*₆): 63.7 (CH₂C=O), 67.9 (CH₂OC=O), 118.9, 122.6, 123.4, 125.9, 129.5, 130.5, 134.4, 137.0, 139.7, 152.6, 159.9, 163.9, 166.3, 169.4 (C₅H₃N, C₅H₄N), 177.8 (CH₂OC=O), 209.7, 214.4 (C≡O), 262.8 (CH₂C=O) ppm.

Attempted H₂ activation by model complex **2** in the presence of Ph₃B

A yellow solution of complex **2** (10 mg, 0.024 mmol) and Ph₃B (5.8 mg, 0.024 mmol) in acetone-*d*₆ (0.50 mL) was added to an NMR tube by a syringe and then a mixture of H₂ and D₂ in ca. 1:1 molar ratio was sparged through the solution for 3 min to give a sample solution, which was analyzed immediately by ¹H NMR spectroscopy. ¹H NMR (400 MHz, acetone-*d*₆): 2.07 (s,

3H, CH₃), 3.93, 4.58 (dd, J = 19.6 Hz, 2H, CH₂C=O), 4.54 (s, H₂), 4.73, 5.41 (dd, J = 13.6 Hz, 2H, CH₂OC=O), 6.77 (d, J = 8.0 Hz, 1H, 3-H of C₅H₄N), 6.99 (t, J = 6.4 Hz, 1H, 5-H of C₅H₄N), 7.35 (t, J = 7.2 Hz, 2H, (C₆H₅)₃B), 7.41–7.49 (m, 8H, (C₆H₅)₃B), 7.55 (d, J = 7.6 Hz, 1H, 4-H of C₅H₄N), 7.62–7.67 (m, 2H, 1H of (C₆H₅)₃B, 3-H of C₅H₃N), 7.79 (d, J = 6.8 Hz, 4H, (C₆H₅)₃B), 7.88 (d, J = 6.8 Hz, 1H, 5-H of C₅H₃N), 8.00 (t, J = 7.6 Hz, 1H, 4-H of C₅H₃N), 8.35 (d, J = 5.2 Hz, 1H, 6-H of C₅H₄N) ppm.

Attempted H₂ activation by model complex 4 in the presence of Ph₃B

The same procedure was followed as that described above, except that complex 4 (10 mg, 0.021 mmol) and Ph₃B (5.0 mg, 0.021 mmol) were utilized instead of the corresponding materials. The ¹H NMR data for this sample solution are as follows. ¹H NMR (400 MHz, acetone-*d*₆): 3.96, 4.62 (dd, J = 19.6 Hz, 2H, CH₂C=O), 4.54 (s, H₂), 4.97, 5.80 (dd, J = 14.0 Hz, 2H, CH₂OC=O), 6.77–6.82 (m, 2H, 3-H of C₅H₄N, 1H of (C₆H₅)₃B), 6.96 (t, J = 6.0 Hz, 1H, 5-H of C₅H₄N), 7.14–7.20 (m, 1H, 4-H of C₅H₄N), 7.35–7.56 (m, 10H, 2H of C₆H₅, 8H of (C₆H₅)₃B), 7.65–7.71 (m, 4H, 2H of C₆H₅, 2H of (C₆H₅)₃B), 7.80 (d, J = 6.8 Hz, 3H, 3H of (C₆H₅)₃B), 7.88 (d, J = 7.2 Hz, 1H, 3-H of C₅H₃N), 8.02–8.09 (m, 3H, 1H of C₆H₅, 5-H of C₅H₃N, 1H of (C₆H₅)₃B), 8.26 (t, J = 7.2 Hz, 1H, 4-H of C₅H₃N), 8.46 (d, J = 4.4 Hz, 1H, 6-H of C₅H₄N) ppm.

X-ray structure determinations of 1–4

Single-crystals of 1–4 suitable for X-ray diffraction analyses were grown by slow evaporation of their CH₂Cl₂/hexane solutions at 0 °C. All the single-crystals were mounted on a Rigaku MM-007 (rotating anode) diffractometer equipped with a Saturn 724 CCD. Data were collected at 113 K using a confocal monochromator with Mo-Kα₁ radiation (λ = 0.71073 Å) in the ω - ϕ scanning

mode. Data collection, reduction, and absorption correction were performed with the CRYSTALCLEAR program.⁴⁵ The structures were solved by direct methods using the SHELXS-97 program⁴⁶ and refined by full-matrix least-squares techniques (SHELXL-97)⁴⁷ on F^2 . Hydrogen atoms were located by using the geometric method. Details of crystal data, data collections, and structure refinements are summarized in Table 4.

Table 4 Crystal data and structure refinements details for **1–4**

	1	2	3	4
Formula	C ₁₂ H ₁₀ FeINO ₅	C ₁₇ H ₁₄ FeN ₂ O ₅ S	C ₁₇ H ₁₂ FeINO ₅	C ₂₂ H ₁₆ FeN ₂ O ₅ S
M_w	430.96	414.21	493.03	476.28
T (K)	113(2)	113(2)	113(2)	113(2)
Cryst syst	Monoclinic	Monoclinic	Monoclinic	Monoclinic
space group	$C2/c$	$P2(1)/n$	$P2(1)/n$	$P2(1)/c$
a (Å)	50.70(2)	8.404(4)	12.505(5)	8.9860(18)
b (Å)	7.723(4)	20.146(9)	8.365(3)	18.680(4)
c (Å)	14.397(7)	10.462(5)	17.836(7)	12.028(2)
α (°)	90	90	90	90
β (°)	92.112(7)	105.231(9)	109.982(6)	90.99(3)
γ (°)	90	90	90	90
V (Å ³)	5633(5)	1708.9(15)	1753.4(11)	2018.7(7)
Z	16	4	4	4
Crystal Size/mm	0.20 × 0.18 × 0.12	0.20 × 0.12 × 0.10	0.20 × 0.18 × 0.12	0.20 × 0.18 × 0.12
D_c (g cm ⁻³)	2.033	1.610	1.868	1.567
μ (mm ⁻¹)	3.280	1.036	2.647	0.889
$F(000)$	3328	848	960	976
Reflns collected	20808	17703	16626	16568
Reflns unique	6684	4047	4173	3558
$\theta_{\min/\max}$ (°)	2.41/27.90	2.02/27.90	1.74/27.90	2.01/25.02
Final R	0.0204	0.0270	0.0189	0.0519
Final R_w	0.0462	0.0738	0.0373	0.1363
GOF on F^2	0.992	1.041	0.995	1.112
$\Delta\rho_{\max/\min}/e \text{ Å}^{-3}$	0.678/−0.958	0.339/−0.449	0.369/−0.375	2.460/−0.645

Electrochemical and electrocatalytic experiments

A solution of 0.1 M *n*-Bu₄NPF₆ in MeCN (Fisher Chemicals, HPLC grade) was used as electrolyte in each of electrochemical and electrocatalytic experiments. The electrolyte solutions

were degassed by bubbling with N₂ for at least 10 min before measurements. The measurements were made using a BAS Epsilon potentiostat. Cyclic voltammograms were obtained in a three-electrode cell with a 3 mm diameter glassy carbon working electrode, a platinum counter electrode and an Ag/Ag⁺ (0.01 M AgNO₃/0.1 M *n*-Bu₄NPF₆ in MeCN) reference electrode under an atmosphere of nitrogen. The working electrode was polished with 0.05 μm alumina paste and sonicated in water for 10 min. Bulk electrolyses were run on a vitreous carbon rod (*A* = 2.9 cm²) in a two-compartment, gastight, H-type electrolysis cell containing ca. 10 mL of MeCN. All potentials are quoted against Fc/Fc⁺ potential. Gas chromatography was performed with a Shimadzu gas chromatograph GC-2014 under isothermal conditions with nitrogen as a carrier gas and a thermal conductivity detector.

Acknowledgements

We are grateful to the National Basic Research Program of China (2014CB845604) and the National Natural Science Foundation of China (21132001, 21272122) for financial support.

References

- 1 R. Cammack, *Nature*, 1999, **397**, 214-215.
- 2 M. W. W. Adams and E. I. Stiefel, *Science*, 1998, **282**, 1842-1843.
- 3 J. A. Wright, P. J. Turrell and C. J. Pickett, *Organometallics*, 2010, **29**, 6146-6156.
- 4 M. Y. Darensbourg, E. J. Lyon and J. J. Smee, *Coord. Chem. Rev.*, 2000, **206-207**, 533-561.
- 5 J. C. Fontecilla-Camps, A. Volbeda, C. Cavazza and Y. Nicolet, *Chem. Rev.*, 2007, **107**, 4273-4303.
- 6 C. Tard and C. J. Pickett, *Chem. Rev.*, 2009, **109**, 2245-2274.
- 7 M. J. Corr and J. A. Murphy, *Chem. Soc. Rev.* 2011, **40**, 2279-2292.
- 8 K. M. Shultz, D. Chen and X. Hu, *Chem. Asian J.*, 2013, **8**, 1068-1075.
- 9 (a) R. K. Thauer, *Microbiology*, 1998, **144**, 2377-2406; (b) C. Zirngibl, R. Hedderich and R.

- K. Thauer, *FEBS Lett.*, 1990, **261**, 112-116.
- 10 E. J. Lyon, S. Shima, R. Boecher, R. K. Thauer, F. W. Grevels, E. Bill, W. Roseboom and S. P. J. Albracht, *J. Am. Chem. Soc.*, 2004, **126**, 14239-14248.
- 11 S. Shima, E. J. Lyon, R. K. Thauer, B. Mienert and E. Bill, *J. Am. Chem. Soc.*, 2005, **127**, 10430-10435.
- 12 S. Shima, S. Vogt, A. Göbels and E. Bill, *Angew. Chem. Int. Ed.*, 2010, **49**, 9917-9921.
- 13 S. Shima, O. Pilak, S. Vogt, M. Schick, M. S. Stagni, W. Meyer-Klaucke, E. Warkentin, R. K. Thauer and U. Ermler, *Science*, 2008, **321**, 572-575.
- 14 T. Hiromoto, K. Ataka, O. Pilak, S. Vogt, M. S. Stagni, W. Meyer-Klaucke, E. Warkentin, R. K. Thauer, S. Shima and U. Ermler, *FEBS Lett.*, 2009, **583**, 585-590.
- 15 T. Hiromoto, E. Warkentin, J. Moll, U. Ermler and S. Shima, *Angew. Chem. Int. Ed.*, 2009, **48**, 6457-6460.
- 16 Y. Guo, H. Wang, Y. Xiao, S. Vogt, R. K. Thauer, S. Shima, P. I. Volkers, T. B. Rauchfuss, V. Pelmeshnikov, D. A. Case, E. E. Alp, W. Sturhahn, Y. Yoda and S. P. Cramer, *Inorg. Chem.*, 2008, **47**, 3969-3977.
- 17 X. Wang, Z. Li, X. Zeng, Q. Luo, D. J. Evans, C. J. Pickett and X. Liu, *Chem. Commun.*, 2008, 3555-3557.
- 18 T. Liu, B. Li, C. V. Popescu, A. Bilko, L. M. Pérez, M. B. Hall and M. Y. Darensbourg, *Chem. Eur. J.*, 2010, **16**, 3083-3089.
- 19 A. M. Royer, T. B. Rauchfuss and D. L. Gray, *Organometallics*, 2009, **28**, 3618-3620.
- 20 A. M. Royer, M. Salomone-Stagni, T. B. Rauchfuss and W. Meyer-Klaucke, *J. Am. Chem. Soc.*, 2010, **132**, 16997-17003.
- 21 P. J. Turrell, J. A. Wright, J. N. T. Peck, V. S. Oganessian and C. J. Pickett, *Angew. Chem. Int. Ed.*, 2010, **49**, 7508-7511.
- 22 D. Chen, R. Scopelliti and X. Hu, *J. Am. Chem. Soc.*, 2010, **132**, 928-929.
- 23 D. Chen, R. Scopelliti and X. Hu, *Angew. Chem. Int. Ed.*, 2010, **49**, 7512-7515.
- 24 D. Chen, R. Scopelliti and X. Hu, *Angew. Chem. Int. Ed.*, 2011, **50**, 5671-5673.
- 25 D. Chen, R. Scopelliti and X. Hu, *Angew. Chem. Int. Ed.*, 2012, **51**, 1919-1921.
- 26 B. Hu, D. Chen and X. Hu, *Chem. Eur. J.*, 2013, **19**, 6221-6224.
- 27 L.-C. Song, Z.-J. Xie, M.-M. Wang, G.-Y. Zhao and H.-B. Song, *Inorg. Chem.*, 2012, **51**, 7466-7468.

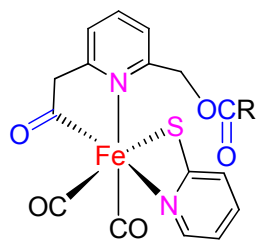
- 28 S. Tanino, Y. Ohki and K. Tatsumi, *Chem. Asian J.*, 2010, **5**, 1962-1964.
- 29 P. J. Turrell, A. D. Hill, S. K. Ibrahim, J. A. Wright and C. J. Pickett, *Dalton Trans.*, 2013, **42**, 8140-8146.
- 30 B. Hu, D. Chen and X. Hu, *Chem. Eur. J.* 2014, **20**, 1677-1682.
- 31 L.-C. Song, G.-Y. Zhao, Z.-J. Xie and J.-W. Zhang, *Organometallics*, 2013, **32**, 2509-2512.
- 32 D. Chong, I. P. Georgakaki, R. Mejia-Rodriguez, J. Sanabria-Chinchilla, M. P. Soriaga and M. Y. Darensbourg, *Dalton Trans.*, 2003, 4158-4163.
- 33 L.-C. Song, Z.-Y. Yang, H.-Z. Bian, Y. Liu, H.-T. Wang, X.-F. Liu and Q.-M. Hu, *Organometallics*, 2005, **24**, 6126-6135.
- 34 J.-F. Capon, F. Gloaguen, P. Schollhammer and J. Talarmin, *Coord. Chem. Rev.*, 2005, **249**, 1664-1676.
- 35 S. J. Borg, T. Behrsing, S. P. Best, M. Razavet, X. Liu and C. J. Pickett, *J. Am. Chem. Soc.*, 2004, **126**, 16988-16999.
- 36 G. A. N. Felton, C. A. Mebi, B. J. Petro, A. K. Vannucci, D. H. Evans, R. S. Glass and D. L. Lichtenberger, *J. Organomet. Chem.*, 2009, **694**, 2681-2699.
- 37 S. Kaur-Ghumaan, L. Schwartz, R. Lomoth, M. Stein and S. Ott, *Angew. Chem. Int. Ed.*, 2010, **49**, 8033-8036.
- 38 G. J. Baird, S. G. Davies and T. R. Maberly, *Organometallics*, 1984, **3**, 1764-1765.
- 39 G. C. Welch and D. W. Stephan, *J. Am. Chem. Soc.*, 2007, **129**, 1880-1881.
- 40 D. Sellmann and A. Fürsattel, *Angew. Chem.*, 1991, **111**, 2142-2145.
- 41 F. A. Jalón, B. R. Manzano, A. Caballero, M. C. Carrión, L. Santos, G. Espino and M. Moreno, *J. Am. Chem. Soc.*, 2005, **127**, 15364-15365.
- 42 E. N. Wayland, *Organic Syntheses*, Wiley, New York, 1988, Coll. Vol. 6, p.807-814.
- 43 T. Z. Zhang and E. V. Anslyn, *Tetrahedron*, 2004, **60**, 11117-11124.
- 44 R. Rathore, C. L. Burns and I. A. Guzei, *J. Org. Chem.*, 2004, **69**, 1524-1530.
- 45 *CrystalClear and Crystalstructure*, Rigaku and Rigaku Americas, The Woodlands, TX, 2007.
- 46 G. M. Sheldrick, *SHELXS97, A Program for Crystal Structure Solution*, University of Göttingen, Germany, 1997.
- 47 G. M. Sheldrick, *SHELXL97, A Program for Crystal Structure Refinement*, University of Göttingen, Germany, 1997.

The Graphical Contents Entry

Synthesis, structural characterization, and some properties of 2-acylmethyl-6-ester group-difunctionalized pyridine-containing iron complexes related to active site of [Fe]-hydrogenase

Li-Cheng Song,* Fu-Qiang Hu, Miao-Miao Wang, Zhao-Jun Xie, Kai-Kai Xu, and Hai-Bin Song

The first four acylmethyl/ester group-disubstituted pyridine-containing models for [Fe]-hydrogenase have been synthesized. While the structures of the four models are confirmed by X-ray crystallography, two of the models are electrochemically studied by CV techniques.



(R = Me, Ph)

Two target model complexes